INVASION GENERATES PERIODIC TRAVELING WAVES (WAVETRAINS) IN PREDATOR-PREY MODELS WITH NONLOCAL DISPERSAL*

JONATHAN A. SHERRATT†

Abstract. Periodic Traveling waves (wavetrains) have been studied extensively in systems of reaction-diffusion equations. An important motivation for this work is the identification of periodic Traveling waves of abundance in ecological data sets. However, for many natural populations diffusion is a poor representation of movement, and spatial convolution with a dispersal kernel is more realistic because of its ability to reflect rare long-distance dispersal events. In marked contrast to the literature on reaction-diffusion systems, there has been almost no previous work on periodic Traveling waves in models with nonlocal dispersal. In this paper the author considers the generation of such waves by the invasion of the unstable coexistence state in cyclic predator-prey systems with nonlocal dispersal for which the dispersal kernel is thin-tailed (exponentially bounded). The main result is formulae for the wave period and amplitude when the parameters of the local population dynamics are close to a Hopf bifurcation point. This result is tested via detailed comparison of the dependence on parameters of the stability of the periodic Traveling waves generated by invasion. The paper concludes with a comparison between the predictions of the nonlocal model and the corresponding reaction-diffusion model. Specifically, the parameter regions giving stable and unstable waves are shown to be the same to leading order close to a Hopf bifurcation point, irrespective of the choice of dispersal kernel.

1. Introduction. Periodic Traveling wave (PTW) solutions of reaction-diffusion equations have been studied since the 1970s [1]. At that time the main foci of research were the existence and stability of PTWs and applications to oscillatory chemical reactions. Mechanisms by which PTWs might arise naturally in applications were first studied in the 1990s, in particular the generation of PTWs behind invasive fronts [2, 3, 4]. Shortly after this, new ecological data sets revealed PTWs of abundance in some cyclic populations [5, 6]. Consequently there has been a large body of subsequent research on PTW generation by biological invasions. This includes work on applications to fungal colonies [7], tumor growth [8], and cell populations [9], but by far the largest body of literature concerns systems of predators and their prey [4, 10, 11, 12, 13, 14, 15, 16, 17]. In parallel with this theoretical research, field studies are revealing PTWs in an increasingly wide range of natural populations, including voles [18, 19], moths [20], and red grouse [21]. To my knowledge, there is no definitive evidence for the origin of the PTWs in any of these systems, but invasion is a clear contender in many cases.

The dominant model formalism used for studying PTWs in ecological systems has been reaction-diffusion equations. However, for many ecological populations, spatial convolution is more realistic than diffusion as a representation of dispersal. Empirical data on many plant and animal species reveal rare long-distance dispersal events, and these can be reflected in a quantifiable way in dispersal kernels. Methods for

†Department of Mathematics and Maxwell Institute for Mathematical Sciences, Heriot-Watt University, Edinburgh EH14 4AS, UK (j.a.sherratt@hw.ac.uk).

kernel estimation include tracking of dispersing individuals (e.g., [22]), mark-recapture (e.g., [23]), and, for plants, genotyping of individual seedlings to determine the source plant (e.g., [24]). The review paper [25] gives a comprehensive list of populations for which kernels have been estimated using such methods.

In [26] I studied the existence and stability of PTW solutions of equations with nonlocal dispersal and with oscillatory kinetics of "λ–ω" type (defined below). To my knowledge that is the only study of PTWs in autonomous models in which dispersal is represented by an integral term, and in the present paper I will extend that work to study PTW generation in both λ–ω and predator-prey models with nonlocal dispersal. However it is important to comment that there is a relatively large literature on PTWs in reaction-diffusion models with nonlocal terms in the kinetics. This includes equations in which intraspecific competition terms involve spatial convolutions [27, 28] and those with nonlocal delays [29, 30, 31]. Of particular note is that in contrast to the local case, scalar reaction-diffusion equations with nonlocal kinetics can have PTW solutions [28]. Of particular relevance to the present paper is the work of Merchant and Nagata [32, 33] on PTWs in predator-prey models with nonlocal prey competition; this will be discussed in more detail below. Finally, some authors have studied PTWs in integrodifferential equation models for populations in landscapes that vary periodically in space or time [34, 35], although here the wave periodicity simply reflects the periodic variation in the parameters.

Predator-prey models typically have three spatially uniform equilibria: the trivial state with no predators or prey, a prey-only state, and a coexistence state. Cyclic population dynamics arise when the last of these loses stability via a Hopf bifurcation. These local dynamics lead to the consideration of two different invasion scenarios: invasion of the prey-only state by predators, and invasion of the coexistence state by oscillatory behavior. The first of these is the most important but also the most complicated. When the coexistence state is stable, one expects simple invasive transition fronts, and their existence has been proved for a number of models [36, 37, 38]. However, for cyclic populations numerical simulations (e.g., [4, 13, 16]) reveal a rich variety of behaviors. This includes "point-to-periodic" fronts in which the front is followed by a wavetrain moving in parallel with it; a PTW behind the front moving with a different speed and in some cases in the opposite direction; a band of PTWs behind the front, followed by spatiotemporal disorder; and spatiotemporal disorder immediately behind the front. In addition, the coexistence state can appear as a permanent spatiotemporal transient behind the front, separating it from the spatiotemporal oscillations. Even for the much-studied case of reaction-diffusion models, our understanding of these phenomena remains very incomplete. It is known that in some cases a "point-to-periodic" invasive front exists [39, 40, 41], and it is known that close to Hopf bifurcation, the point-to-point invasive transition front exists and remains stable, with the spatiotemporal oscillations in the wake of the front being separated from the front interface [42, 43]. Beyond this there are no precise results, although a number of authors have attempted to understand the complex array of behaviors using formal or approximate methods. In particular, in [44] I predicted the wavelength of the PTW occurring behind the front when the kinetic parameters are close to Hopf bifurcation, and this approximation was improved significantly in recent work by Merchant and Nagata [16, 33]. Also, the widths of spatiotemporally transient regions of coexistence steady state and PTWs have been estimated using absolute stability theory [45, 46, 47].

In view of this highly incomplete picture of the invasion of the prey-only state by predators for (local) reaction-diffusion models, I will not consider this type of invasion

in my work on the more complicated case of models with nonlocal dispersal—of course, it remains a natural area for future work. Instead I will restrict attention to the invasion of the coexistence state. From the viewpoint of applications, this is relevant when a change in environmental conditions alters the local dynamics from noncyclic to cyclic, so that the coexistence state changes stability: a local disturbance would then initiate an invasion process. For example, in southern Finland the characteristic 3-year cycle in vole abundance disappeared in the mid 1990s, reappearing about 5 years later [48], possibly due to the differing responses of interacting vole species to climate changes. This corresponds to a stabilization and then a destabilization of the coexistence state; unfortunately there is no spatially extended field data for this system. A number of other multiyear population cycles have also collapsed over the last two decades; see [49] for a detailed review. For example, long-standing vole cycles in Kielder Forest (UK) disappeared in the late 1990s; here the cause is thought to be milder winters [18]. In this case there has not been a reappearance of cycles but it seems likely that a series of severe winters would destabilize the noncycling state. The invasion of the coexistence state is also important mathematically. The various studies described above on the invasion of the prey-only state all suggest that the key to understanding this process, and to predicting the wavelength of PTWs generated by invasion, actually lies in invasions of the coexistence state. This is particularly emphasized by the recent work of Merchant and Nagata [16, 33].

The main result of the present paper is a prediction of the wavelength and amplitude of the PTW generated by the invasion of the coexistence steady state for parameter values close to a Hopf bifurcation point in the local population dynamics. The outline of the paper is as follows. In section 2 I describe the predator-prey model used, and I present the results of numerical simulations. In sections 3 and 4 I consider behavior close to a Hopf bifurcation in the local population dynamics; in that case I am able to make analytical predictions of the selected PTW and its stability. In section 5 I discuss numerical tests of these predictions in the case of a dispersal kernel of Laplace type, for which the two nonlocal equations can be rewritten as a system of four (local) partial differential equations; this enables a more detailed numerical investigation of PTW solutions. In section 6 I make a quantitative comparison between the nonlocal predator-prey model and the corresponding (local) reaction-diffusion model, focusing on the regions in parameter space giving stable and unstable PTWs behind invasion. Finally in section 7 I discuss the implications of my results and highlight some key questions for future work.

2. Numerical simulations of invasion of the predator-prey coexistence state. The approach used in this paper is not restricted to particular predator-prey kinetics, but for the purposes of specific illustration I will use the Rosenzweig–MacArthur model [50], augmented by nonlocal dispersal:

$$
\text{(2.1a)} \quad \boxed{\text{predators}} \quad \frac{\partial p}{\partial t} = \overbrace{\int_{y=-\infty}^{y=+\infty} K(x-y)p(y,t)dy - p}^{\text{dispersal}} + \overbrace{(C/B)hp/(1+Ch)}^{\substack{\text{benefit from} \\ \text{predation}}} - \overbrace{p/AB}^{\text{death}},
$$

$$
\text{(2.1b)} \quad \boxed{\text{prey}} \quad \frac{\partial h}{\partial t} = \underbrace{\int_{y=-\infty}^{y=+\infty} K(x-y)h(y,t)dy - h}_{\text{dispersal}} + \underbrace{h(1-h)}_{\substack{\text{intrinsic} \\ \text{birth \& death}}} - \underbrace{\frac{Cph}{1+Ch}}_{\text{predation}}.
$$

These equations are nondimensional with $p(x,t)$ and $h(x,t)$ denoting predator and prey densities at space point x and time t; throughout the paper I will consider only

one-dimensional spatial domains. The local population dynamics make the simple assumptions of logistic prey growth, an increasing saturating rate of prey consumption per predator, a birth rate of predators that is proportional to this consumption, and a constant per capita predator death rate. For mathematical simplicity I assume that the two populations disperse at the same rate. This is appropriate for most aquatic systems, but many terrestrial predators disperse more rapidly than their prey, and potential extensions to unequal dispersal are discussed in section 7. The dispersal kernel $K(y)$ must be ≥ 0 for all y and must satisfy $\int_{-\infty}^{+\infty} K(y)\,dy = 1$ so that the dispersal term conserves population. I assume that $K(.)$ is even, corresponding to unbiased dispersal; an important case for which an asymmetric kernel would be appropriate is a population living in a river [51]. Also, I will restrict attention to kernels that are "thin-tailed," i.e., exponentially bounded, using as particular examples the Laplace and Gaussian kernels,

$$(2.2) \qquad \text{Laplace kernel:} \quad K(s) = (1/2a)\exp\big(-|s|/a\big),$$

$$(2.3) \qquad \text{Gaussian kernel:} \quad K(s) = \big(1/a\sqrt{\pi}\big)\exp\big(-s^2/a^2\big),$$

$(a > 0)$, which are probably the most widely used kernels in ecological and epidemiological applications (e.g., [51, 52, 53]). Note that I exclude from consideration kernels that are "fat-tailed." These are used in many ecological applications [25, 54, 55], especially in the context of invasion fronts (e.g., [56]). A detailed study of PTWs for such kernels is an important issue for future work, but in [26] I showed that for the commonly used Cauchy kernel all nontrivial PTWs are unstable, suggesting that PTWs may not be an important solution form for populations that disperse via fat-tailed kernels.

Equations (2.1) have three homogeneous steady states: trivial $p = h = 0$; prey-only $p = 0$, $h = 1$; and coexistence $p = Ah_s(1 - h_s)$, $h = h_s \equiv 1/[C(A - 1)]$. The last of these is unstable when $A > 1$ and $C > (A+1)/(A-1)$, with a stable limit cycle [57]. Figure 1 shows typical numerical simulations of the invasion of the coexistence state when it is unstable, following a localized disturbance. An invasion front moves across the domain, leaving behind it either PTWs (Figure 1(a)) or a band of PTWs followed by spatiotemporal irregularity (Figure 1(b)). It is important to comment that I have not proved the existence of PTWs for (2.1) and this is a natural area for future work. However, numerical results such as those in Figure 1 strongly suggest existence.

My numerical results are qualitatively the same as those found in numerical simulations of reaction-diffusion predator-prey models [59, 60, 61], where the irregular oscillations develop when the PTW selected behind the invasion is unstable. However, the details of PTW selection for general parameters remain unclear even for reaction-diffusion models, and in this paper I will focus on behavior close to Hopf bifurcation, that is, when C is slightly greater than $(A + 1)/(A - 1)$. In this case I will derive an approximation to the selected PTW.

3. Invasions in $\boldsymbol{\lambda}$–$\boldsymbol{\omega}$ systems. Close to a Hopf bifurcation in the local dynamics, (2.1) can be approximated by the appropriate normal form. For oscillatory reaction-diffusion equations and a wide range of other spatially extended oscillatory systems, the normal form is the complex Ginzburg–Landau equation [62, 63]. However, for systems with nonlocal spatial coupling a different, nonlocal normal form is
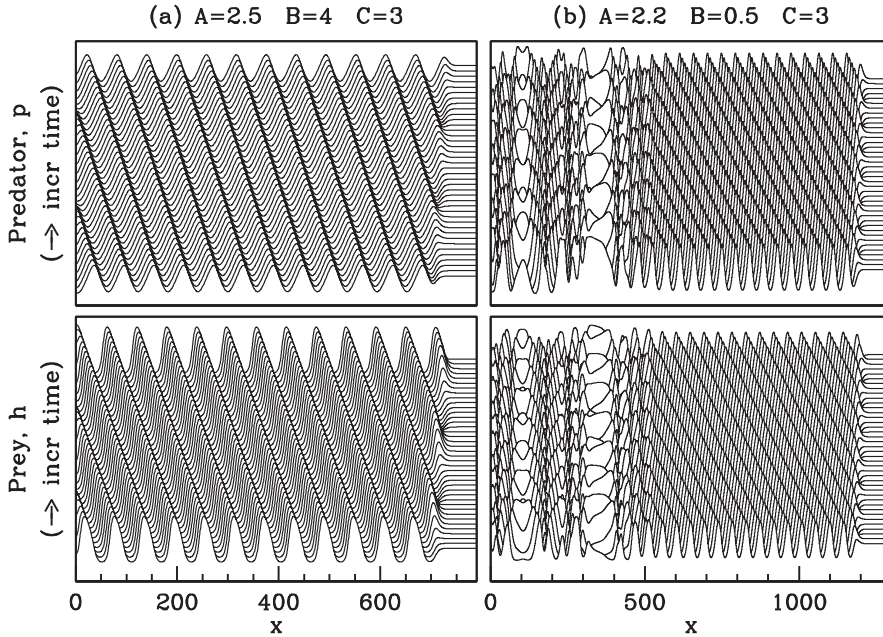
FIG. 1. *Examples of* PTW *generation in the predator-prey model* (2.1). *In* (a) *the selected* PTW *is stable, while in* (b) *it is unstable so that one sees a band of* PTWs *immediately behind the invasion, followed by spatiotemporal disorder. I show space-time plots for predator and prey densities when* (a) $2500 \leq t \leq 2580$, (b) $5500 \leq t \leq 5580$; *the vertical separation of the solutions is proportional to the time interval. The equations were solved numerically by discretizing in space using a uniform grid* ($\delta x = 0.5$) *and solving the resulting system of* ODEs *using the stiff* ODE *solver* ROWMAP [58] *(http:// numerik.mathematik.uni-halle.de/forschung/software/), with relative and absolute error tolerances both set to* 10^{-8}. *The* ODE *system includes a numerical calculation of the spatial convolutions using fast Fourier transforms. To avoid the difficulties posed by boundaries with non-Dirichlet conditions, my simulations actually involved invasions initiated by a local perturbation in the center of the domain (at* $x = 0$); *the solutions are plotted for* $x > 0$ *only.*

needed [64, 65, 66, 67], and for (2.1) this is

$$\partial u/\partial t = \int_{y=-\infty}^{y=+\infty} K(x-y)u(y,t)dy - u + (\lambda_0 - \lambda_1 r^2)u - (\omega_0 + \omega_1 r^2)v,$$

(3.1)

$$\partial v/\partial t = \int_{y=-\infty}^{y=+\infty} K(x-y)v(y,t)dy - v + (\omega_0 + \omega_1 r^2)u + (\lambda_0 - \lambda_1 r^2)v.$$

Here $r = \sqrt{u^2 + v^2}$ and λ_0, λ_1, ω_0, and ω_1 are constants with $\lambda_0, \lambda_1 > 0$. The "λ–ω" kinetics in (3.1) are the same as in the complex Ginzburg–Landau equation, which has been widely studied in both the applied mathematics [68] and the physics [63] literature. In (3.1) $u = v = 0$ corresponds to the coexistence steady state of the predator-prey model (2.1), and Figure 2 shows two numerical simulations of invasions of this steady state, following a localized disturbance. As expected, the solution for u (and for v) shows a clear resemblance to the predator-prey solutions in Figure 1. Moreover, plots of the amplitude r and phase gradient $\partial\theta/\partial x$ (where $\theta = \tan^{-1}(v/u)$) have the form of transition fronts moving with constant shape and speed (middle and lower panels of Figure 2). This solution form is the key to predicting the PTW that is selected by the invasion.
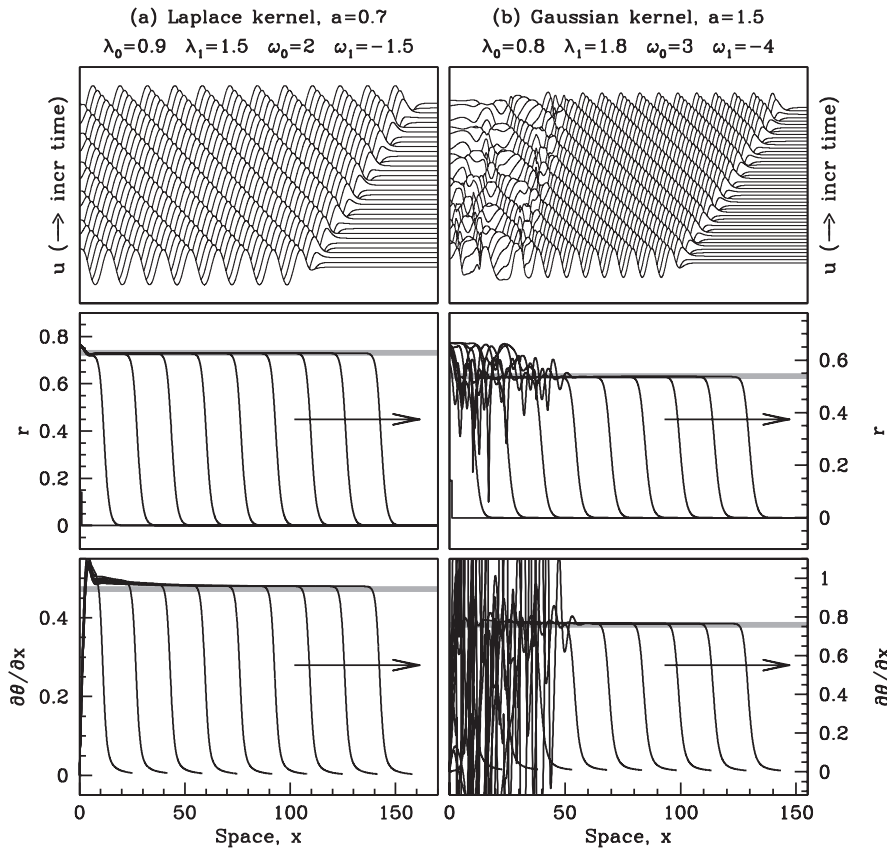
FIG. 2. *Examples of* PTW *generation in the* λ–ω *equations* (3.1). *In* (a) *the selected* PTW *is stable, while in* (b) *it is unstable so that one sees a band of* PTWs *immediately behind the invasion, followed by spatiotemporal disorder. The upper panels show space-time plots for* u *when* $70 \le t \le 100$, *with the vertical separation of the solutions being proportional to the time interval; the corresponding solutions for* v *are qualitatively the same but with a phase difference in the oscillations. The middle panels show the amplitude* r *as a function of space* x *at times* $t = 10, 20, 30, \ldots, 100$. *The thick gray line indicates the amplitude predicted by the calculations in section 4. The lower panels show the corresponding solutions for the phase gradient* $\partial\theta/\partial x$; *this is not defined when* $r = 0$ *and is plotted only when the numerical solution for* r *exceeds* 10^{-5}. *In these panels the thick gray line indicates the wavenumber predicted by the calculations in section 4. Equations* (3.1) *were solved numerically as described in the legend of Figure* 1, *with a uniform space mesh of width* 0.05 *and with the absolute and relative error tolerances in* ROWMAP *set to* 10^{-10}.

Specifically, I will prove the following, which is the main result of the paper.

THEOREM 3.1. *Suppose that* (3.1) *has a solution of the form* $r(x,t) = \tilde{r}(z) > 0$ *and* $\theta_x = \tilde{\psi}(z)$, *where* $z = x - ct$ *with* $c > 0$ *constant, and with*

$$\tilde{r}(z) \to R, \quad \tilde{r}'(z) \to 0, \quad \tilde{\psi}(z) \to \alpha \text{ as } z \to -\infty,$$
$$\tilde{r}(z) \sim r_0 e^{-\xi z}, \quad \tilde{\psi}(z) \sim \psi_0 e^{-\xi z} \text{ as } z \to \infty,$$

where $R > 0$, $r_0 > 0$, *and* $\psi_0 \neq 0$. *Suppose also that* $K(.)$ *is even with* $K(s) \le K_0 e^{-\theta|s|}$ *when* $|s|$ *is sufficiently large for some* $K_0 > 0$ *and some* $\theta > \xi$. *Then*

(i) α *satisfies*

(3.2)
$$c\,\alpha = (\omega_1/\lambda_1)\left[1 - \lambda_0 - \int_{s=-\infty}^{s=+\infty} K(s)\cos(\alpha s)\,ds\right]$$

(ii) *to leading order as $z \to \infty$, $\tilde{r}(z)$ satisfies*

$$c\,\frac{\partial \tilde{r}}{\partial z} + \int_{\zeta=-\infty}^{\zeta=+\infty} K(z-\zeta)\,\tilde{r}(\zeta)\,d\zeta + (\lambda_0 - 1)\tilde{r} = 0\,.$$

To avoid confusion, I remark that I use the notation $f_1(z) \sim f_2(z)$ as $z \to \infty$ to mean that $f_1(z)/f_2(z) \to 1$.

The appropriate value of c is suggested by work on spreading speeds in simpler equations. For the scalar integrodifferential equation

(3.3a)
$$\frac{\partial w}{\partial t} = \int_{y=-\infty}^{y=+\infty} K(x-y)w(y,t)dy - w + f(w)$$

(3.3b)
$$\text{with } f(0) = f(1) = 0, \quad f'(0) > 0, \quad f'(1) < 0,$$

spreading speeds were first considered by Medlock and Kot [52], who argued intuitively that for localized disturbances to the $w = 0$ state, the spreading speed of the disturbance will be $\min_{\eta>0}(1/\eta)\left[M(\eta) - 1 + f'(0)\right]$; I denote by $\eta_{\min}$ the value of η at which this minimum occurs. Here the moment generating function $M(\eta) = \int_{s=-\infty}^{s=+\infty} K(s)e^{\eta s}\,ds$. The arguments of Medlock and Kot [52] also indicate that the tail of the wave front decays to zero in proportion to $e^{-\eta_{\min}z}$.

These intuitively based results were subsequently proved by Lutscher, Pachepsky, and Lewis [51] given suitable assumptions on $f(.)$ and $K(.)$, and then by Zhang, Li, and Wang [69] for more general functions. For systems of integrodifferential equations, the only results on spreading speeds that I am aware of concern SIR epidemic models [70]. In particular, there is to my knowledge no theory for the spreading speed in (3.1). However, Theorem 3.1(ii) implies that linearizing (3.1) about $u = v = 0$ gives an integrodifferential equation for r that corresponds exactly with the linearization of (3.3) about $w = 0$. This suggests that for invasion in λ–ω systems, the appropriate value of the invasion speed c is

(3.4)
$$c = \min_{\eta>0}\mathcal{C}(\eta), \quad \text{where } \mathcal{C}(\eta) = (1/\eta)\left[M(\eta) - 1 + \lambda_0\right]\,.$$

Moreover, the value of ξ in the statement of the theorem will be $\eta_{\min}$. Typically the set $\mathcal{S} := \{\eta \mid M(\eta) \text{ is defined}\}$ is either the whole real line or an open subset; this is assumed, for example, in the work of Lutscher, Pachepsky, and Lewis [51], and it holds for both the Laplace and Gaussian kernels. Then $\xi = \eta_{\min} \in \mathcal{S}$, and also there is a $\theta \in \mathcal{S}$ that is $> \xi$, as required for Theorem 3.1. I cannot prove (3.4) but I have confirmed it in numerical simulations for a wide range of parameter values, for the Laplace and Gaussian kernels.

Taken together, (3.2) and (3.4) can be solved for α, the value of $\partial\theta/\partial x$ behind the invasion. Solutions of (3.1) with constant $r = R$ and $\partial\theta/\partial x = \alpha$ are periodic Traveling waves, with the form

$$u = R\cos\left[\alpha x + \left(\omega_0 + \omega_1 R^2\right)t\right], \quad v = R\sin\left[\alpha x + \left(\omega_0 + \omega_1 R^2\right)t\right]$$

[26]. Moreover R is given in terms of α by

$$(3.5) \qquad R = \left[(1/\lambda_1) \left(\lambda_0 - 1 + \int_{s=-\infty}^{s=+\infty} K(s) \cos(\alpha s) \right) \right]^{1/2}$$

[26]. Therefore the determination of the value of α behind the invasion solves the PTW selection problem. In section 4 I will illustrate this by constructing explicit solutions for the cases of Laplace and Gaussian kernels, and I will compare my results with those from numerical simulations. In the remainder of this section I present a proof of Theorem 3.1. The main difficulty in the proof is the delicate limiting behavior of the various improper integrals near the two asymptotes of the transition front.

Proof of Theorem 3.1.

Stage 1: *Formulating the Traveling wave equations.* I begin by rewriting (3.1) in terms of $r(x,t) = \left(u^2 + v^2 \right)^{1/2}$ and $\theta(x,t) = \tan^{-1}(v/u)$, which gives

$$(3.6a) \quad \frac{\partial r}{\partial t} = \int_{y=-\infty}^{y=+\infty} K(x-y) r(y,t) \cos\big[\theta(y,t) - \theta(x,t)\big]\, dy + (\lambda_0 - 1)r - \lambda_1 r^3,$$

$$(3.6b) \quad \frac{\partial \theta}{\partial t} = \int_{y=-\infty}^{y=+\infty} K(x-y) \frac{r(y,t)}{r(x,t)} \sin\big[\theta(y,t) - \theta(x,t)\big]\, dy + \omega_0 + \omega_1 r^2 .$$

The solution form given in the statement of the theorem is $r = \tilde{r}(z)$ and $\theta = \tilde{\Psi}(z) + \theta_0(t)$, where $\tilde{\Psi}(.)$ is an integral of $\tilde{\psi}(.)$. Substituting this into (3.6) implies that $d\theta_0/dt$ is a constant, say, $\theta_0 = \theta_1 t + \theta_2$, with the Traveling wave equations being

$$(3.7a) \qquad 0 = c\frac{d\tilde{r}}{dz} + \mathcal{I} + (\lambda_0 - 1)\tilde{r} - \lambda_1 \tilde{r}^3,$$

$$(3.7b) \qquad 0 = c\tilde{\psi} - \theta_1 + \mathcal{J} + \omega_0 + \omega_1 \tilde{r}^2 ,$$

$$(3.7c) \qquad \mathcal{I} = \int_{\zeta=-\infty}^{\zeta=+\infty} K(z-\zeta)\, \tilde{r}(\zeta) \cos\big[\tilde{\Psi}(\zeta) - \tilde{\Psi}(z)\big]\, d\zeta ,$$

$$(3.7d) \qquad \mathcal{J} = \int_{\zeta=-\infty}^{\zeta=+\infty} K(z-\zeta) \frac{\tilde{r}(\zeta)}{\tilde{r}(z)} \sin\big[\tilde{\Psi}(\zeta) - \tilde{\Psi}(z)\big]\, d\zeta .$$

Stage 2: *Form of* (3.7a) *as* $z \to -\infty$. Consider a function $\sigma(z) > 0$ such that $\sigma(z)$ and $|z| - \sigma(z)$ both $\to \infty$ as $z \to \pm\infty$. Later in the proof I will impose a tighter restriction on $\sigma(z)$. I then define $\rho(z) = \sup_{s \geq -\sigma(z)} |\tilde{r}(z-s) - R|$ and $\delta(z) = \sup_{s \geq -\sigma(z)} |\tilde{\psi}(z-s) - \alpha|$. Note that the limiting behaviors $z + \sigma(z) \to -\infty$, $\tilde{r}(z) \to R$, and $\tilde{\psi}(z) \to \alpha$ as $z \to -\infty$ together imply that $\rho(z)$ and $\delta(z) \to 0$.

My basic approach is to use the behavior of (3.7a) as $z \to -\infty$ to deduce a relationship between R and α. The difficulty lies in determining the behavior of $\mathcal{I}$ in this limit. I will investigate this by splitting the domain of integration into two parts: $\zeta < z + \sigma(z)$ and $\zeta > z + \sigma(z)$. The limiting behavior of the first part can be resolved using the property $\sigma(z) \to \infty$ as $z \to -\infty$, while for the second part I use $z + \sigma(z) \to -\infty$.

Using the triangle inequality, $\left| \mathcal{I} - R \int_{s=-\infty}^{s=\infty} K(s) \cos(\alpha s) \, ds \right| \leq \mathcal{I}_1 + \mathcal{I}_2 + \mathcal{I}_3$, where

$$\mathcal{I}_1 = \left| \int_{s=-\infty}^{s=-\sigma(z)} K(s) \tilde{r}(z-s) \cos\big[\tilde{\Psi}(z-s) - \tilde{\Psi}(z)\big] \, ds \right|,$$

$$\mathcal{I}_2 = \left| \int_{s=-\sigma(z)}^{s=\infty} K(s) \tilde{r}(z-s) \cos\big[\tilde{\Psi}(z-s) - \tilde{\Psi}(z)\big] \, ds - R \int_{s=-\sigma(z)}^{s=\infty} K(s) \cos(\alpha s) \, ds \right|,$$

$$\mathcal{I}_3 = \left| R \int_{s=-\infty}^{s=-\sigma(z)} K(s) \cos(\alpha s) \, ds \right|.$$

Now $\mathcal{I}_1 \leq \int_{s=-\infty}^{s=-\sigma(z)} K(s) \tilde{r}(z-s) \, ds$. Since $\tilde{r}(z)$ is defined for all z and tends to finite limits as $z \to \pm\infty$, it is bounded, say, $\tilde{r}(z) \leq C_1$ for all z. Thus $\mathcal{I}_1 \leq C_1 \int_{s=-\infty}^{s=-\sigma(z)} K(s) \, ds$. This integral converges for all z since $K(.)$ is exponentially bounded. Moreover $\sigma(z) \to \infty$ as $z \to -\infty$. Therefore $\mathcal{I}_1 \to 0$ as $z \to -\infty$. Similarly $\mathcal{I}_3 \to 0$ as $z \to -\infty$.

I turn now to the more difficult case of $\mathcal{I}_2$, which can be rewritten as

$$\mathcal{I}_2 = \int_{s=-\sigma(z)}^{s=\infty} K(s) \big| \underbrace{\tilde{r}(z-s)}_{p_1} \underbrace{\cos\big[\tilde{\Psi}(z-s) - \tilde{\Psi}(z)\big]}_{q_1} - \underbrace{R}_{p_2} \underbrace{\cos(\alpha s)}_{q_2} \big| \, ds.$$

I use the inequality $|p_1 q_1 - p_2 q_2| \leq |q_1| \cdot |p_1 - p_2| + |p_2| \cdot |q_1 - q_2|$ with the p_i's and q_i's as indicated. Noting that $|\tilde{r}(z-s) - R| \leq \rho(z)$ throughout the range of integration, this gives

$$(3.8) \quad \mathcal{I}_2 \leq \rho(z) \int_{s=-\sigma(z)}^{s=\infty} K(s) \, ds + R \int_{s=-\sigma(z)}^{s=\infty} K(s) \left| \cos\big[\tilde{\Psi}(z-s) - \tilde{\Psi}(z)\big] - \cos(\alpha s) \right| \, ds.$$

Since the derivative of $\cos(.)$ is ≤ 1 in absolute value, the mean value theorem implies

$$\left| \cos\big[\tilde{\Psi}(z-s) - \tilde{\Psi}(z)\big] - \cos(\alpha s) \right| = \left| \cos\big[\tilde{\Psi}(z-s) - \tilde{\Psi}(z)\big] - \cos(-\alpha s) \right|$$
$$\leq \left| \tilde{\Psi}(z-s) - \tilde{\Psi}(z) + \alpha s \right|,$$

and applying the mean value theorem again gives

$$\left| \tilde{\Psi}(z-s) - \tilde{\Psi}(z) + \alpha s \right| \leq \left| (-s) \left[\tilde{\psi}(z - \tau s) - \alpha \right] \right| \text{ for some } \tau \in (0,1)$$
$$\leq |s| \delta(z) \text{ for all } s \geq -\sigma(z).$$

Also $\int_{s=-\sigma(z)}^{s=\infty} K(s) \, ds \leq \int_{s=-\infty}^{s=\infty} K(s) \, ds = 1$. Hence (3.8) implies that $\mathcal{I}_2 \leq \rho(z) + \delta(z) R \int_{s=-\infty}^{s=\infty} K(s) |s| \, ds$. The kernel $K(.)$ is exponentially bounded, and thus the integral in this expression converges. Since $\rho(z)$ and $\delta(z)$ both $\to 0$ as $z \to -\infty$, $\mathcal{I}_2 \to 0$ also.

I have shown that $\mathcal{I} \to R \int_{s=-\infty}^{s=\infty} K(s) \cos(\alpha s) \, ds$ as $z \to -\infty$. Since $\tilde{r}'(z) \to 0$ and $\tilde{r}(z) \to R$ in this limit, (3.7a) implies that $\lambda_0 - 1 - \lambda_1 R^2 + \int_{s=-\infty}^{s=\infty} K(s) \cos(\alpha s) \, ds = 0$.

Stage 3: *Form of* (3.7b) *as* $z \to -\infty$. For (3.7b) the basic difficulty in determining behavior as $z \to -\infty$ again lies in the integral term. A directly analogous methodology to that used above for $\mathcal{I}$ shows that as $z \to -\infty$, $\mathcal{J} \to \int_{s=-\infty}^{s=\infty} K(s) \sin(\alpha s) \, ds = 0$

since $K(.)$ is even. The only new feature in the proof of this limit, compared to that for $\mathcal{I}$, is that one must consider the term $\big([\tilde{r}(z-s)/\tilde{r}(z)]-1\big)$ in an integral with respect to s with limits $s = -\sigma(z)$ and $s = \infty$. For this, I note that throughout the range of integration and for z sufficiently large and negative, $R - \rho(z) \leq \tilde{r}(z)$, $\tilde{r}(z-s) \leq R + \rho(z)$. Also, for z sufficiently large and negative, $\rho(z) \leq \frac{1}{2}R$. Together these imply $\big| [\tilde{r}(z-s)/\tilde{r}(z)] - 1 \big| \leq (4/R)\rho(z)$. With the addition of this inequality, the argument used above for the limiting value of $\mathcal{I}$ can be extended directly to $\mathcal{J}$. The limiting form of (3.7b) as $z \to -\infty$ then follows immediately:

$$c\,\alpha - \theta_1 + \omega_0 + \omega_1 R^2 = 0.$$

Stage 4: *Value of* θ_1. It remains to determine the value of the constant θ_1, which follows from a consideration of the limiting behavior of the Traveling wave equations (3.7) as $z \to \infty$. I will show that $\mathcal{J} \to 0$ in this limit, from which it follows that $\theta_1 = \omega_0$. I split the integral $\mathcal{J}$ into three parts, $\mathcal{J} = \mathcal{J}_1 + \mathcal{J}_2 + \mathcal{J}_3$, where

$$\mathcal{J}_1 = \int_{s=-\infty}^{s=-\sigma(z)} K(s)\frac{\tilde{r}(z-s)}{\tilde{r}(z)} \sin\big[\tilde{\Psi}(z-s) - \tilde{\Psi}(z)\big]\, ds,$$

$$\mathcal{J}_2 = \int_{s=-\sigma(z)}^{s=\sigma(z)} K(s)\frac{\tilde{r}(z-s)}{\tilde{r}(z)} \sin\big[\tilde{\Psi}(z-s) - \tilde{\Psi}(z)\big]\, ds,$$

$$\mathcal{J}_3 = \int_{s=\sigma(z)}^{s=\infty} K(s)\frac{\tilde{r}(z-s)}{\tilde{r}(z)} \sin\big[\tilde{\Psi}(z-s) - \tilde{\Psi}(z)\big]\, ds\,.$$

I consider first $\mathcal{J}_1$. I have $\tilde{r}(z) \sim r_0 e^{-\xi z} \Rightarrow \tilde{r}(z) \geq C_2 e^{-\xi z}$ for sufficiently large z, and also $\tilde{r}(z-s) \leq C_3 e^{-\xi(z-s)} \leq C_3 e^{-\xi(z+\sigma(z))}$ for $s \leq -\sigma(z)$, again for sufficiently large z. Here C_2 and C_3 are suitably chosen positive constants. Also $K(s) \leq K_0 e^{\theta s}$ throughout the range of integration, for sufficiently large z. Combining these gives

$$|\mathcal{J}_1| \leq (C_3 K_0/C_2)e^{-\xi\sigma(z)} \int_{s=-\infty}^{s=-\sigma(z)} e^{\theta s}\, ds = (C_3 K_0/\theta C_2)e^{-(\xi+\theta)\sigma(z)} \to 0 \text{ as } z \to \infty\,.$$

For $\mathcal{J}_3$ a similar argument can be used with one important difference. For s in this range of integration $\tilde{r}(z-s)$ may or may not approach zero as $z \to \infty$; however, I argued above that $\tilde{r}(.)$ is bounded. Hence throughout the range of integration $\tilde{r}(z-s) \leq C_1$. Also, as for $\mathcal{J}_1$, provided that z is sufficiently large $\tilde{r}(z) \geq C_2 e^{-\xi z}$, and also $K(s) \leq K_0 e^{-\theta s}$ throughout the range of integration. Therefore

$$(3.9) \qquad |\mathcal{J}_3| \leq (C_1 K_0/C_2)e^{\xi z} \int_{s=\sigma(z)}^{s=\infty} e^{-\theta s}\, ds = (C_1 K_0/\theta C_2)e^{(\xi z - \theta\sigma(z))}\,.$$

Thus far, the choice of $\sigma(z)$ has been arbitrary within the constraints that $\sigma(z)$ and $|z| - \sigma(z) \to \infty$ as $z \to \pm\infty$. I now make the more specific assumption that $\sigma(z) = \gamma|z|$ with $1 > \gamma > \xi/\theta$. Then (3.9) implies that $\mathcal{J}_3 \to 0$ as $z \to \infty$.

I will now show that $\mathcal{J}_2$ also $\to 0$ as $z \to \infty$. This requires consideration of the sin function in the integrand. I define $\mu(z) = \sup_{s \leq \sigma(z)}\big|\tilde{\psi}(z-s)\big|$. Since $z - \sigma(z) \to \infty$ and $\tilde{\psi}(z) \to 0$ as $z \to \infty$, $\mu(z) \to 0$. The mean value theorem implies that for some $\tau \in (0,1)$, $\big|\tilde{\Psi}(z-s) - \tilde{\Psi}(z)\big| \leq |s| \cdot \big|\tilde{\psi}(z-\tau s)\big| \leq \mu(z)|s|$; this holds for all $s \leq \sigma(z)$. Since the derivative of $\sin(.)$ is ≤ 1 in absolute value, applying the mean value theorem again gives $\big|\sin\big[\tilde{\Psi}(z-s) - \tilde{\Psi}(z)\big]\big| \leq \mu(z)|s|$. Turning attention to the $\tilde{r}(z-s)/\tilde{r}(z)$ term, for sufficiently large z we have $\tilde{r}(z) \geq C_4 e^{-\xi z}$ and also $\tilde{r}(z-s) \leq$

$C_5 e^{\xi(s-z)}$ for any $s \in (-\sigma(z), \sigma(z))$. Here C_4 and C_5 are suitably chosen positive constants. These various inequalities give $|\mathcal{J}_2| \leq (C_5/C_4)\mu(z) \int_{s=-\sigma(z)}^{s=\sigma(z)} |s| K(s) e^{\xi s} \, ds$. Since $K(s) \leq K_0 e^{-\theta|s|}$ for sufficiently large $|s|$ with $\theta > \xi$, the integral in the above expression converges as $z \to \infty$, implying that $\mathcal{J}_2 \to 0$. This completes the proof of part (i) of the theorem.

Stage 5: Linearization of (3.7a) *as* $z \to \infty$. The approach used to prove that $\mathcal{J} \to 0$ as $z \to \infty$ can also be used to prove part (ii) of the theorem, concerning the linearization of (3.7a) ahead of the invasion. Using $\tilde{r}(z-s) \leq C_1$ and $\left|\cos\left[\tilde{\Psi}(z-s) - \tilde{\Psi}(z)\right] - 1\right| \leq 2$ for all z and s,

$$\left| \mathcal{I} - \int_{s=-\infty}^{s=\infty} K(s)\tilde{r}(z-s) \, ds \right| \leq 2C_1 \int_{s=\sigma(z)}^{s=\infty} K(s) \, ds$$
$$+ \int_{s=-\infty}^{s=\sigma(z)} K(s)\tilde{r}(z-s) \cdot \left| 1 - \cos[\tilde{\Psi}(z-s) - \tilde{\Psi}(z)] \right| ds \,.$$

For sufficiently large s, $K(s) \leq K_0 e^{-\theta s} \Rightarrow 2C_1 \int_{s=\sigma(z)}^{s=\infty} K(s) \, ds \leq 2(C_1 K_0/\theta) e^{-\theta \sigma(z)}$ for sufficiently large z. I have shown above that $\left| \tilde{\Psi}(z-s) - \tilde{\Psi}(z) \right| \leq \mu(z)|s|$ for $s \leq \sigma(z)$ and z sufficiently large; also $\tilde{r}(z-s) \leq C_3 e^{-\xi(z-s)}$. Using the standard inequality $1 - \cos\phi \leq \frac{1}{2}\phi^2$ (valid for all ϕ) it follows that

$$\int_{-\infty}^{\sigma(z)} K(s)\tilde{r}(z-s) \cdot \left| 1 - \cos\left[\tilde{\Psi}(z-s) - \tilde{\Psi}(z)\right] \right| ds \leq \tfrac{1}{2} C_3 \mu(z)^2 e^{-\xi z} \int_{-\infty}^{\sigma(z)} K(s) e^{\xi s} s^2 \, ds$$
$$\leq \tfrac{1}{2} C_3 \mu(z)^2 e^{-\xi z} \int_{-\infty}^{\infty} K(s) e^{\xi s} s^2 \, ds$$
$$\leq C_6 \mu(z)^2 e^{-\xi z}$$

for some $C_6 > 0$ as a result of the asymptotic behavior of $K(s)$ as $s \to \pm\infty$. Also $\tilde{\psi}(z) \sim \psi_0 e^{-\xi z}$ as $z \to \infty \Rightarrow \mu(z) \sim |\psi_0| e^{-\xi(z-\sigma(z))}$. Combining these results gives

(3.10) $$\left| \mathcal{I} - \int_{s=-\infty}^{s=\infty} K(s)\tilde{r}(z-s) \, ds \right| \leq 2(C_1 K_0/\theta) e^{-\theta \sigma(z)} + C_7 e^{-3\xi z + 2\xi \sigma(z)}$$

for some $C_7 > 0$.

As $z \to \infty$ both $\mathcal{I}$ and $\int_{s=-\infty}^{s=\infty} K(s)\tilde{r}(z-s) \, ds \to 0$. To obtain the linearization of (3.7a) ahead of the wave, it is necessary to augment (3.10) with a careful estimate of $\int_{s=-\infty}^{s=\infty} K(s)\tilde{r}(z-s) \, ds$ for large z. To do this, I recall that $C_2 e^{-\xi(z-s)} \leq \tilde{r}(z-s) \leq C_3 e^{-\xi(z-s)}$ for all $s \leq \sigma(z)$, when z is sufficiently large. Also $K(s) \leq K_0 e^{-\theta|s|}$ when $|s|$ is sufficiently large. Therefore for sufficiently large z, $\int_{s=-\infty}^{s=\infty} K(s)\tilde{r}(z-s) \, ds$ lies in

$$\left[C_2 e^{-\xi z} \int_{s=-\infty}^{s=\sigma(z)} K(s) e^{\xi s} \, ds \,,\, C_3 e^{-\xi z} \int_{s=-\infty}^{s=\sigma(z)} K(s) e^{\xi s} \, ds + K_0 \int_{s=\sigma(z)}^{s=\infty} e^{-\theta s}\tilde{r}(z-s) \, ds \right]$$
$$\subseteq \left[C_2 e^{-\xi z} \int_{s=-\infty}^{s=0} K(s) e^{\xi s} \, ds \,,\, C_3 e^{-\xi z} \int_{s=-\infty}^{s=\infty} K(s) e^{\xi s} \, ds + (C_1 K_0/\theta) e^{-\theta \sigma(z)} \right] \,.$$

The asymptotic form of $K(s)$ as $s \to \pm\infty$ implies convergence of the integrals of $K(s) e^{\xi s}$ on $(-\infty, 0)$ and $(-\infty, \infty)$. Moreover both integrals must be strictly positive. Therefore for suitable $C_8, C_9 > 0$

(3.11) $$C_8 e^{-\xi z} \leq \int_{s=-\infty}^{s=\infty} K(s)\tilde{r}(z-s) \, ds \leq C_9 e^{-\xi z} + (C_1 K_0/\theta) e^{-\theta \sigma(z)} \,.$$

Thus far I have assumed that $\sigma(z) = \gamma|z|$ with $1 > \gamma > \xi/\theta$. I now tighten this restriction, requiring $1 > \gamma > 3\xi/(2\xi + \theta)$. Then $e^{-\theta\sigma(z)} \ll e^{-\xi z}$ and $e^{-\theta\sigma(z)} \ll e^{-3\xi z + 2\xi\sigma(z)}$ as $z \to \infty$. Therefore (3.10) implies that

$$\left| \mathcal{I} - \int_{s=-\infty}^{s=\infty} K(s)\tilde{r}(z-s)\, ds \right| \leq C_{10} e^{-\xi z} e^{-2(1-\gamma)\xi z}$$

for some $C_{10} > 0$ when z is sufficiently large, while (3.11) gives

$$C_8 e^{-\xi z} \leq \int_{s=-\infty}^{s=\infty} K(s)\tilde{r}(z-s)\, ds \leq C_{11} e^{-\xi z}$$

for some $C_{11} > 0$. Therefore $\mathcal{I} \sim \int_{s=-\infty}^{s=\infty} K(s)\tilde{r}(z-s)\, ds$ as $z \to \infty$, which completes the proof of part (ii) of the theorem.

4. PTW selection in λ–ω systems for Laplace and Gaussian kernels. To illustrate the PTW selection implied by (3.2) and (3.4), and to enable numerical verification of my results, I now consider the specific cases of kernels of Laplace (2.2) and Gaussian (2.3) types.

4.1. Laplace kernel. For the Laplace form (2.2) of the kernel $K(.)$, PTW solutions of (3.1) are discussed in detail in [26]. Briefly, there is a one-to-one relationship between wavenumber α and amplitude R: $\lambda_0 - \lambda_1 R^2 = a^2\alpha^2/(1 + a^2\alpha^2)$. If $\lambda_0 \geq 1$ there are PTWs for all values of α, while if $\lambda_0 < 1$, then α must be $\leq [\lambda_0/(1-\lambda_0)]^{1/2}/a$, with the amplitude R being 0 at this maximum wavenumber. PTW stability is also determined in [26]: PTWs are unstable/stable when $|\alpha|$ is above/below $\alpha_L^{\text{stab}} \in \left(0, \frac{1}{a\sqrt{3}}\right)$, which is the unique solution of an algebraic equation given in [26].

For this kernel, the moment generating function $M(\eta) = 1/(1 - a^2\eta^2)$ (valid for $|\eta| < 1/a$). Using this, (3.4) gives $c = a\kappa_L$, where κ_L is an (algebraically complicated) function of λ_0. Turning to (3.2), the integral $\int_{s=-\infty}^{s=+\infty} K(s)\cos(\alpha s)\, ds = 1/(1 + \alpha^2 a^2)$ and thus α satisfies

(4.1) $$\kappa_L \alpha a = (\omega_1/\lambda_1)\left[1 - \lambda_0 - 1/(1 + \alpha^2 a^2)\right].$$

To consider solutions of (4.1), suppose first that $\omega_1 > 0$. Since $\lambda_1 > 0$, the left- and right-hand sides of (4.1) are respectively increasing and decreasing functions of α on $\alpha < 0$, and their values at $\alpha = 0$ and $-\infty$ imply that there is exactly one solution for α in this range. The possibility of positive solutions must also be considered. If $\lambda_0 > 1$ this can be ruled out immediately because the right-hand side of (4.1) is always negative. If $\lambda_0 < 1$, then (4.1) can in fact have solutions with $\alpha > 0$. However, PTWs are restricted to $\alpha < [\lambda_0/(1 - \lambda_0)]^{1/2}/a$, and in this range (and with $\alpha > 0$) the right-hand side of (4.1) is negative so that no solutions are possible. Directly analogous arguments apply when $\omega_1 < 0$.

Thus (4.1) has exactly one solution for α, which has the opposite sign to ω_1. This solution can be above or below α_L^{stab}, implying that the selected PTW can be either stable or unstable. Figure 2(a) shows an example of the former case. The invasion leaves a PTW in its wake whose wavenumber and amplitude match the predicted solution for α and the corresponding value of R.

4.2. Gaussian kernel. For $K(.)$ given by (2.3), PTW solutions of (3.1) are again discussed in detail in [26]. Again there is a one-to-one relationship between wavenumber α and amplitude R, in this case given by $\lambda_0 - \lambda_1 R^2 = 1 - \exp(-\alpha^2 a^2/4)$. Again

if $\lambda_0 \geq 1$ there are PTWs for all values of α, while if $\lambda_0 < 1$ there is a maximum possible value of α, corresponding to $R = 0$: $(2/a)\left[\log\left(1/(1-\lambda_0)\right)\right]^{1/2}$. PTWs are unstable/stable when $|\alpha|$ is above/below a critical value $\alpha_G^{\text{stab}} \in \left(0, \sqrt{2}/a\right)$, which is the unique solution of an algebraic equation given in [26].

As for the Laplace kernel, there is a unique solution of (3.2), (3.4) for α in this case, whose sign is opposite to that of ω_1. The argument justifying this is directly analogous to that for the Laplace kernel, and I give only a brief summary. Equation (3.4) gives $c = a\kappa_G$, where $\kappa_G > 0$ depends on λ_0. Then (3.2) implies

$$(4.2) \qquad (\lambda_1/\omega_1)\,\kappa_G\alpha a = \left[1 - \lambda_0 - e^{-\alpha^2 a^2/4}\right].$$

When α and ω_1 have opposite signs, one side of (4.2) is increasing with the other decreasing, as functions of α, and there is exactly one solution. When the signs are the same, the left-hand side of (4.2) is positive, while the right-hand side is negative for all α if $\lambda_0 > 1$ and for all $\alpha < (2/a)\left[\log\left(1/(1-\lambda_0)\right)\right]^{1/2}$ if $\lambda_0 < 1$.

Again the solution for α can be above or below α_G^{stab}, implying that the selected PTW can be either stable or unstable. Figure 2(b) shows an example of the latter case. A PTW develops behind the invasion and then destabilizes, giving irregular spatiotemporal oscillations. Again, the wavenumber and amplitude of the PTW match the predicted solution for α and the corresponding value of R. Note that in reaction-diffusion equations with λ–ω kinetics, the width of the band of PTWs immediately behind the invasion front can be determined using the theory of absolute and convective instabilities [45, 47]. For integrodifferential equations there is currently no corresponding theory, and this is a natural target for future research.

5. Comparison of PTW selection in predator-prey and λ–ω systems. For given predator-prey kinetics, the appropriate coefficients λ_0, λ_1, ω_0, and ω_1 can be determined by the standard process of reduction to normal form [71]. For (2.1) this process is described in detail in [13] and [72], and online supplements to those papers contain MAPLE worksheets that perform the derivation, with C treated as the bifurcation parameter. The results are

$$(5.1a) \qquad \lambda_0 = \frac{(A-1)C - (A+1)}{2A(A+1)}, \qquad \lambda_1 = \frac{A+1}{4A},$$

$$(5.1b) \qquad \omega_0 = \left(\frac{A-1}{AB(A+1)}\right)^{1/2} + \frac{\left[(A-1)C - (A+1)\right](A-1)^{1/2}}{2A^{3/2}(A+1)^{3/2}B^{1/2}}$$

$$(5.1c) \quad \omega_1 = \frac{(A+1)^{1/2}\left(2A^2+5AB-A^5B-A^4-4A^3B+2A^2-4A^2B^2+5AB-1\right)}{24[A^7(A-1)B^3]^{1/2}}.$$

These formulae enable quantitative comparisons between numerical results for (2.1) and my analytical results for (3.1). Such comparisons are most effective if one can compare not only predictions of the existence and selection of PTWs but also predictions of their stability. To my knowledge there is currently no methodology by which one can determine the stability of a PTW solution of a general integrodifferential equation such as (2.1), even numerically. However, for the special case of the Laplace kernel (2.2) there is a standard trick via which (2.1) can be reduced to a system of (local) partial differential equations. Standard numerical methods are then available to test PTW stability, and this approach was used previously by Merchant and Nagata [33] in their study of PTWs in a reaction-diffusion predator-prey model with

nonlocal prey competition. Using the notation $P(x,t) = \int_{y=-\infty}^{y=+\infty} K(x-y)p(y,t)dy$ and $H(x,t) = \int_{y=-\infty}^{y=+\infty} K(x-y)h(y,t)dy$, (2.1) can be rewritten as

$$\text{(5.2a)} \qquad \partial p/\partial t = P + (C/B)hp/(1+Ch) - (1+1/AB)p,$$

$$\text{(5.2b)} \qquad \partial h/\partial t = H - h^2 - Cph/(1+Ch),$$

$$\text{(5.2c)} \qquad 0 = \partial^2 P/\partial x^2 + (p-P)/a^2,$$

$$\text{(5.2d)} \qquad 0 = \partial^2 H/\partial x^2 + (h-H)/a^2.$$

I used the software package WAVETRAIN [73], which uses numerical continuation to determine the existence and stability of PTW solutions of partial differential equations. In (5.2), the branches of PTW solutions start at Hopf bifurcation points in the Traveling wave ODEs, and WAVETRAIN traces these branches numerically to determine PTW existence. For stability, WAVETRAIN calculates the spectrum of a PTW by numerical continuation, starting from eigenfunctions with the same periodicity as the PTW– these can be approximated by solving a matrix eigenvalue problem [74]. The absence of time derivatives in (5.2c), (5.2d) means that this matrix eigenvalue problem is of generalized type [75]. WAVETRAIN can also track the boundary between stable and unstable PTWs in a parameter plane, by numerically continuing parameter pairs at which either the spectrum has zero curvature at the origin (Eckhaus points) or the spectrum touches the imaginary axis away from the origin (Hopf points) [75].

The normal form coefficients (5.1) apply when C is regarded as the bifurcation parameter; recall that the kinetics have a Hopf bifurcation at $C = (A+1)/(A-1)$. Therefore it is most convenient to consider the dependence of PTWs on the parameter B, with fixed values of A and C. Figure 3 illustrates the results of investigations of this type, with $A = 2$ and $C = 3.5, 3.1,$ and 3.02; the Hopf bifurcation occurs at $C = 3$. The figure shows wavelength *vs* B. I plot the minimum wavelength for PTWs and the stability boundaries, both as calculated numerically for (5.2) (dashed curves) and as obtained using my analytical results for (3.1) with (5.1) (solid curves). For both loci the analytical approximations and numerical calculations approach one another as C approaches the Hopf bifurcation value, as expected. WAVETRAIN identifies the stability boundary as being of Eckhaus type, as predicted by my analysis in [26] of PTW stability for (3.1),(2.2). I also plot my prediction of the PTW selected by invasion in (3.1), (2.2), (5.1) and the wavelength of the PTWs that develop in numerical simulations of invasion in (2.1). Again, the two approach one another as C approaches $(A+1)/(A-1)$. In keeping with the form of the stability boundaries, my numerical simulations show a band of PTWs followed by spatiotemporal irregularities when B is either small or large, but only PTWs at intermediate B (Figures 3(d)–(f)). Note that when the selected wave is unstable but close to the stability boundary, the band of PTWs is very wide, and irregularities only occur on a large spatial domain.

6. Comparison of PTW stability in local and nonlocal predator-prey models. My numerical simulations (Figures 1, 2, 3(d)–(f)) demonstrate a strong qualitative similarity between PTW generation in models with nonlocal dispersal and in reaction-diffusion models. However, my analytical work enables a more quantitative comparison. A natural approach to this is to consider the stability of the PTW selected by the invasion process close to Hopf bifurcation, as a function of the kinetic parameters A and B. To begin I choose $\epsilon > 0$. Then for given values of $A > 1$ and B, I take $C = (1+\epsilon)(A+1)/(A-1)$; recall that $(A+1)/(A-1)$ is the Hopf bifurcation point in the local population dynamics. I then calculate the coefficients $\lambda_0, \lambda_1, \omega_0,$ and ω_1 using (5.1), and I use (3.2) and (3.4) to determine the wavenumber
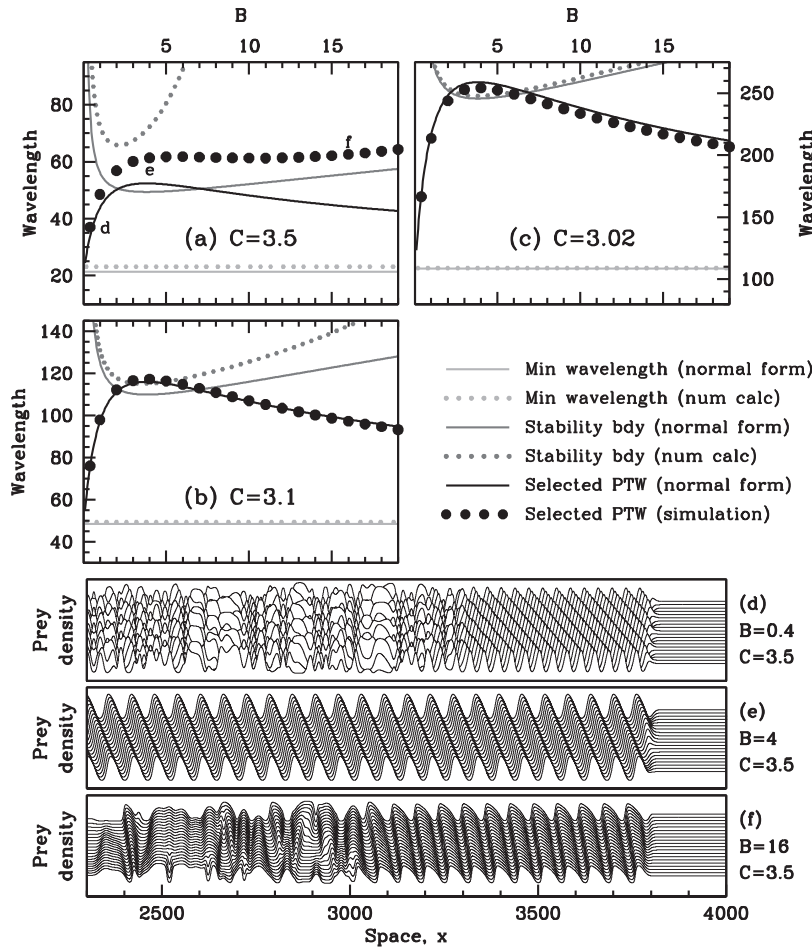
FIG. 3. (a)–(c) *Comparison of numerical results on* PTWs *and analytical results from the normal form approximation, for the Laplace dispersal kernel* (2.2). *The parameter* $A = 2$ *in all cases, so that the Hopf bifurcation in the kinetics occurs at* $C = 3$. *Three types of curve are plotted: the locus of Hopf bifurcation points in the Traveling wave equations, which gives the minimum wavelength for* PTWs *to exist; the stability boundary, above which* PTWs *are stable; and the locus of* PTWs *selected by invasion. All three of these curves are calculated analytically in section 4.1 for the normal form equations. The minimum wavelength and the stability boundary were calculated numerically for* (5.2) *using the software package* WAVETRAIN, *as described in the main text. The wavelength selected by invasion was calculated by numerical simulation: details of my numerical method are given in the legend of Figure* 1. *Numerical convergence tests show that the error arising from the spatial discretization is proportional to* δx^2. *I calculated the wavelength for* $\delta x = 0.5$ *and* $\delta x = 0.25$ *and then used Richardson extrapolation to obtain a more accurate wavelength estimate. Note that the variable time-stepping used by* ROWMAP *makes it impossible to use convergence acceleration to reduce the temporal component of the error; I set both absolute and relative error tolerances to* 10^{-8}. (d)–(f) *Space-time plots of* PTW *generation by invasion for* $C = 3.5$ *and for three different values of* B. *These plots are intended to illustrate the behaviors represented in* (a)–(c), *and the corresponding data points are labeled in* (a). *The simulations are actually run on* $-4000 \leq x \leq 4000$, *with the coexistence steady state perturbed near* $x = 0$ *at time* $t = 0$, *but for greater clarity I show only part of the domain. The solutions are plotted for* $14600 \leq t \leq 14640$, *with time increasing up the page and with the separation of the solutions being proportional to the time interval. In all three cases a* PTW *is generated behind the invasion. In* (d) *and* (f) *the* PTWs *are unstable and occur only as a relatively thin band before destabilizing into spatiotemporal disorder. In* (e) *the* PTW *is also unstable (see* (a)*), but the maximum positive eigenvalue associated with the instability is much smaller and therefore the* PTWs *persist for a much greater distance behind invasion: in fact there is no visible instability even on the full domain* $-4000 \leq x \leq 4000$.
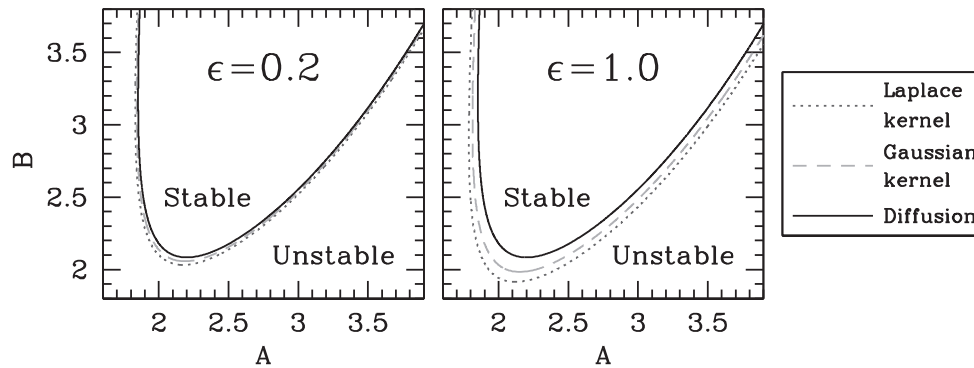
FIG. 4. *Division of the A–B parameter plane into regions for which invasion of the coexistence steady state generates stable and unstable* PTW*s. I show the result for two values of* $\epsilon = C - (A + 1)/(A-1)$*, in each case for nonlocal dispersal with the Laplace and Gaussian kernels and for diffusive dispersal. For given A and B, the stability of the* PTW *selected by invasion can be determined as described in the main text. To calculate the curves shown in the figure, I first calculated stability over a grid of A–B values and then used a numerical equation solver to obtain more accurate locations of the stability boundary.*

of the PTW selected behind invasion. I then test the stability of this PTW using the conditions derived in [26]. Using this approach, one can divide the A–B plane into regions giving stable and unstable PTWs behind invasion. In [13] I implemented this procedure for the reaction-diffusion model with the same local dynamics as in (2.1) but with dispersal represented by scalar linear diffusion; the results are presented in Figure 3 of [13] and are reproduced in Figure 4 here. The selected PTW is unstable for small (close to 1) and large values of A, but (provided that B is greater than about 2) there is a range of intermediate values of A for which the PTW is stable.

For the reaction-diffusion model the stability of the selected wave is independent of ϵ (i.e., of C) and depends only on A and B [13]. This statement requires clarification: what I mean is that within the context of the normal form approximation (3.1), stability is determined by the coefficients λ_1 and ω_1 only, and these are independent of C. Away from the Hopf bifurcation in the local dynamics the stability of the selected PTW does depend on C, but close to Hopf bifurcation this occurs only via higher order terms, beyond the basic λ–ω normal form expansion. However, my calculations in sections 3 and 4 show that for the normal form of the model with nonlocal dispersal (2.1) the selected wave and its stability depend on the coefficient λ_0 (as well as λ_1 and ω_1) and hence on ϵ. Figure 4 shows the boundary in the A–B plane between stable and unstable waves for two different values of ϵ and for the Laplace and Gaussian kernels. Even for the large value of $\epsilon = 1$ the two curves are close to one another and to the stability boundary for the reaction-diffusion model; for small values of ϵ the three curves are almost indistinguishable. This remarkable result implies that provided the kinetic parameters are not too far from the Hopf bifurcation point, there is a close *quantitative* similarity between the predictions of reaction-diffusion models of PTW generation behind invasion and those of models with nonlocal dispersal.

I now explore this quantitative similarity in detail, proving the following result.

THEOREM 6.1. *Consider the generation of* PTW*s in* (2.1) *by an invasion with speed given by* (3.4)*, and suppose that the kernel $K(.)$ is exponentially bounded. Then to leading order as $C \to (A+1)/(A-1)^+$, the condition for the selected* PTW *to be Eckhaus stable is the same as in the corresponding reaction-diffusion model, i.e., the equations with the same local dynamics and scalar diffusion.*

The phrase "Eckhaus stable" means that the PTW is stable to perturbations of sufficiently small wavenumber. For the reaction-diffusion model (with scalar diffusion) corresponding to (3.1) it is known that Eckhaus stability of a PTW implies stability, and in [26] I show that this also holds for (3.1) when the kernel is of Laplace or Gaussian type. However, in general Eckhaus stability does not imply stability for (3.1), even for thin-tailed kernels: a counterexample is given in [26].

Theorem 6.1 implies that to leading order close to Hopf bifurcation, the boundary in parameter space between the generation of stable and unstable PTWs behind invasion is the same whether dispersal is modeled by diffusion or by a spatial convolution for any dispersal kernel for which Eckhaus stability of PTWs implies stability. The intuitive explanation for this can be seen in the proof below: to leading order close to Hopf bifurcation, the Eckhaus stability of the selected PTW in the nonlocal model depends only on the second moment of the kernel, which is the term corresponding to diffusion in a power series expansion.

Proof of Theorem 6.1. If C is close to $(A+1)/(A-1)$, then the leading order behavior can be deduced from (3.1), and λ_0 is small. The selected PTW is given by (3.2) and (3.4); I begin by considering the second of these equations. $\mathcal{C}'(\eta) = 0$ when $\eta \int_{s=-\infty}^{s=\infty} sK(s)e^{\eta s}\,ds + 1 - \int_{s=-\infty}^{s=\infty} K(s)e^{\eta s}\,ds = \lambda_0$. The left-hand side of this equation is strictly positive when $\eta > 0$, implying that at a local minimum $\eta = o(1)$ as $\lambda_0 \to 0$. Since $K(.)$ is exponentially bounded at infinity, the integrals can be expanded as Taylor series in η by differentiating under the integral sign, which shows that $\eta_{\min} = 2\lambda_0^{1/2}/\Gamma + o(\lambda_0^{1/2})$, where $\Gamma = \left(2\int_{s=-\infty}^{s=\infty} s^2 K(s)\,ds\right)^{1/2}$. Substituting this value of η back into (3.4) and expanding as a Taylor series in $\lambda_0^{1/2}$ shows that to leading order the invasion speed $c = \lambda_0^{1/2}\Gamma$.

Considering now (3.2), this implies that α must also $\to 0$ as $\lambda_0 \to 0$, and Taylor series expansion gives

$$(6.1) \qquad \tfrac{1}{4}\Gamma^2\alpha^2 - \lambda_0^{1/2}\left(\lambda_1/\omega_1\right)\Gamma\alpha = \lambda_0 + o(\lambda_0) + o(\lambda_0^{1/2}\alpha) + o(\alpha^2).$$

In [26] I show that the condition for a PTW solution of (3.1) with wavenumber α to be Eckhaus stable is

$$\left[\lambda_0 - 1 + \int_{s=-\infty}^{s=+\infty} K(s)\cos(\alpha s)\,ds\right]\int_{s=-\infty}^{s=+\infty} s^2 K(s)\cos(\alpha s)\,ds$$

$$(6.2) \qquad\qquad\qquad > \left[\int_{s=-\infty}^{s=+\infty} sK(s)\sin(\alpha s)\,ds\right]^2\left(1+\omega_1^2/\lambda_1^2\right).$$

Performing Taylor series expansions in α for all the integrals, this gives $\left(3 + 2\omega_1^2/\lambda_1^2\right)$ $\Gamma^2\alpha^2 < 4\lambda_0 + o(\lambda_0)$. Eliminating α between this inequality and (6.1) gives the leading order condition for stability of the PTW selected behind the invasion as $(\omega_1/\lambda_1)^6 + 2(\omega_1/\lambda_1)^4 - (\omega_1/\lambda_1)^2 < 3$. This is exactly the condition derived in [44] for the stability of PTWs generated by invasion in the reaction-diffusion model with the same kinetics as (3.1) and scalar diffusion, which completes the proof of the theorem. Numerical solution of the cubic polynomial shows that the stability condition is equivalent to $|\omega_1|/\lambda_1 < 1.0714\ldots$; this can be translated into a condition on the parameters A and B using (5.1).

7. Discussion. The generation of PTWs in the wake of invasion in cyclic populations has been predicted by a large number of modeling studies. This includes

simulation-based work using integrodifference equations [11, 76], coupled map lattices [77], and cellular automata [11, 78]. However, the only previous detailed analysis of PTW generation by invasion is for (local) reaction-diffusion models, with the exception of the recent work of Merchant and Nagata on reaction-diffusion models with nonlocal kinetics [32, 33]. A shortcoming of such models is that diffusion is a poor representation of dispersal for many ecological systems; convolution with a dispersal kernel is more realistic because of its ability to reflect occasional long-distance dispersal events [25, 56]. However, the only previous work on PTWs in models with nonlocal dispersal is my recent paper [26], which considers existence and stability of PTWs when the local dynamics are of "λ–ω" type (3.1). In the present paper I have presented the first results on PTW generation by invasion in such models.

As expected from a preliminary study such as this, my work raises many questions for future work, of which I highlight four. First, I have assumed throughout that the dispersal term is the same for predators and prey. Different dispersal coefficients would lead to cross-dispersal terms in the normal form, while different dispersal kernels would give a much more complicated normal form structure. Investigation of PTWs in these cases is an important future challenge. Second, my calculations of PTW selection apply only close to Hopf bifurcation in the local dynamics. Extension of these results to more general parameters is an important research topic, but a challenging one—it remains unsolved even for reaction-diffusion models. However, the recent work of Merchant and Nagata [16, 33] provides a starting point for future study. Third, formal questions of existence and uniqueness remain unexplored for the model (2.1). A number of such results have been proved for models of single populations with nonlocal dispersal [79, 80, 81] but to my knowledge there are no corresponding results for systems. In addition, formal proof of the existence of PTW solutions is a major outstanding problem. Finally, perhaps the most important area for future work is the generation of PTWs by the invasion of the prey-only state, rather than the coexistence state. This is important from the viewpoint of applications but is significantly more difficult from a mathematical viewpoint. However, experience with reaction-diffusion models [13, 16, 33, 44] suggests that the detailed understanding of the invasion of the coexistence state that I have presented will provide an essential precursor to the study of this more complicated invasion process.

REFERENCES

[1] N. KOPELL AND L. N. HOWARD, *Plane wave solutions to reaction-diffusion equations*, Stud. Appl. Math., 52 (1973), pp. 291–328.

[2] J. A. SHERRATT, *On the evolution of periodic plane waves in reaction-diffusion equations of λ–ω type*, SIAM J. Appl. Math., 54 (1994), pp. 1374–1385.

[3] J. A. SHERRATT, *Irregular wakes in reaction-diffusion waves*, Physi. D, 70 (1994), pp. 370–382.

[4] S. V. PETROVSKII, M. E. VINOGRADOV, AND A. Y. MOROZOV, *Spatial-temporal dynamics of a localized populational burst in a distributed prey-predator system*, Okeanologiya, 38 (1998), pp. 881–890.

[5] E. RANTA AND V. KAITALA, *Travelling waves in vole population dynamics*, Nature, 390 (1997), pp. 456–456.

[6] X. LAMBIN, D. A. ELSTON, S. J. PETTY, AND J. L. MACKINNON, *Spatial asynchrony and periodic travelling waves in cyclic populations of field voles*, Proc. R. Soc. Lond. Ser. B, 265 (1998), pp. 1491–1496.

[7] F. A. DAVIDSON, *Chaotic wakes and other wave-induced behavior in a system of reaction-diffusion equations*, Internat J. Bifur. Chaos, 8 (1998), pp. 1303–1313.

[8] I. J. STAMPER, M. R. OWEN, P. K. MAINI, ET AL., *Oscillatory dynamics in a model of vascular tumour growth—implications for chemotherapy*, Biol. Direct, 5 (2010), 27.

[9] A. D. REY AND M. C. MACKEY, *Transitions and kinematics of reaction-convection fronts in a cell population model*, Phys. D, 80 (1995), pp. 120–139.

[10] J. A. SHERRATT, M. A. LEWIS, AND A. C. FOWLER, *Ecological chaos in the wake of invasion*, Proc. Natl. Acad. Sci. USA, 92 (1995), pp. 2524–2528.

[11] J. A. SHERRATT, B. T. EAGAN, AND M. A. LEWIS, *Oscillations and chaos behind predator-prey invasion: Mathematical artifact or ecological reality?*, Philos. Trans. R. Soc. Lond. Ser. Biol. Sci. B, 352 (1997), pp. 21–38.

[12] S. V. PETROVSKII AND H. MALCHOW, *Critical phenomena in plankton communities:* KISS *model revisited*, Nonlinear Anal. Real-world Appl., 1 (2000), pp. 37–51.

[13] J. A. SHERRATT, *Periodic travelling waves in cyclic predator-prey systems*, Ecology Lett., 4 (2001), pp. 30–37.

[14] I. G. PEARCE, M. A. J. CHAPLAIN, P. G. SCHOFIELD, A. R. A. ANDERSON, AND S. F. HUBBARD, *Modelling the spatio-temporal dynamics of multi-species host-parasitoid interactions: Heterogeneous patterns and ecological implications*, J. Theoret Biol., 241 (2006), pp. 876–886.

[15] M. R. GARVIE, *Finite difference schemes for reaction-diffusion equations modeling predator-prey interactions in MATLAB*, Bull. Math. Biol., 69 (2007), pp. 931–956.

[16] S. M. MERCHANT AND W. NAGATA, *Wave train selection behind invasion fronts in reaction-diffusion predator-prey models*, Phys. D, 239 (2010), pp. 1670–1680.

[17] M. R. GARVIE, J. BURKARDT, AND J. MORGAN, *Simple finite element methods for approximating predator-prey dynamics in two dimensions using Matlab*, Bull. Math. Biol., 77 (2015), pp. 547–578.

[18] S. M. BIERMAN, J. P. FAIRBAIRN, S. J. PETTY, D. A. ELSTON, D. TIDHAR, AND X. LAMBIN, *Changes over time in the spatiotemporal dynamics of cyclic populations of field voles (Microtus agrestis L.)*, Am. Nat., 167 (2006), pp. 583–590.

[19] K. BERTHIER, S. PIRY, J. F. COSSON, P. GIRAUDOUX, J. C. FOLTÊTE, R. DEFAUT, D. TRUCHETET, AND X. LAMBIN, *Dispersal, landscape and travelling waves in cyclic vole populations*, Ecol. Lett., 17 (2014), pp. 53–64.

[20] D. M. JOHNSON, O. N. BJØRNSTAD, AND A. M. LIEBHOLD, *Landscape mosaic induces traveling waves of insect outbreaks*, Oecologia, 148 (2006), pp. 51–60.

[21] R. MOSS, D. A. ELSTON, AND A. WATSON, *Spatial asynchrony and demographic travelling waves during red grouse population cycles*, Ecology, 81 (2000), pp. 981–989.

[22] B. T. HIRSCH, M. D. VISSER, R. KAYS, AND P. A. JANSEN, *Quantifying seed dispersal kernels from truncated seed-tracking data*, Meth. Ecol. Evol., 3 (2012), pp. 595–602.

[23] Z. FRIC AND M. KONVICKA, *Dispersal kernels of butterflies: Power-law functions are invariant to marking frequency*, Basic Appl. Ecol., 8 (2007), pp. 377–386.

[24] J. J. ROBLEDO-ARNUNCIO AND C. GARCÍA, *Estimation of the seed dispersal kernel from exact identification of source plants*, Mol. Ecol., 16 (2007), pp. 5098–5109.

[25] R. NATHAN, E. KLEIN, J. J. ROBLEDO-ARNUNCIO, ET AL., *Dispersal kernels: Review*, in Dispersal Ecology and Evolution, J. Clobert, M. Baguette, T. G. Benton, and J. M. Bullock, eds., Oxford University Press, Oxford, UK, 2012, pp. 187–210.

[26] J. A. SHERRATT, *Periodic travelling waves in integrodifferential equations for nonlocal dispersal*, SIAM J. Appl. Dyn. Syst., 13 (2014), pp. 1517–1541.

[27] N. APREUTESEI, A. DUCROT, AND V. VOLPERT, *Travelling waves for integro-differential equations in population dynamics*, Discrete Contin Dyn. Syst. Ser. B, 11 (2009), 541–561.

[28] V. VOLPERT, *Pulses and waves for a bistable nonlocal reaction-diffusion equation*, Appl. Math. Lett., 44 (2015), pp. 21–25.

[29] N. F. BRITTON, *Spatial structures and periodic traveling waves in an integrodifferential reaction-diffusion population model*, SIAM J. Appl. Math., 50 (1990), pp. 1663–1688.

[30] S. A. GOURLEY AND N. F. BRITTON, *Instability of traveling wave solutions of a population model with nonlocal effects*, IMA J. Appl. Math., 51 (1993), pp. 299–310.

[31] D. DUEHRING AND W. Z. HUANG, *Periodic travelling waves for diffusion equations with time delayed and non-local responding reaction*, J. Dynam. Differential Equations, 19 (2007), pp. 457–477.

[32] S. M. MERCHANT AND W. NAGATA, *Instabilities and spatiotemporal patterns behind predator invasions with nonlocal prey competition*, Theor. Pop. Biol., 80 (2011), pp. 289–297.

[33] S. MERCHANT AND W. NAGATA *Selection and stability of wave trains behind predator invasions in a model with non-local prey competition*, IMA J. Appl. Math., in press, `doi:10.1093/imamat/hxu048`.

[34] Y. JIN AND X. Q. ZHAO, *Spatial dynamics of a periodic population model with dispersal*, Nonlinearity, 22 (2009), pp. 1167–1189.

[35] F. LUTSCHER, *Nonlocal dispersal and averaging in heterogeneous landscapes*, Appl. Anal., 89 (2010), pp. 1091–1108.

[36] S. R. DUNBAR, *Travelling wave solutions of diffusive Lotka-Volterra equations: A heteroclinic connection in* R^4, Trans. Amer. Math. Soc., 286 (1984), pp. 557–594.

[37] W. Z. HUANG, *Traveling wave solutions for a class of predator-prey systems*, J. Dynam. Differential Equations, 24 (2012), pp. 633–644.

[38] Y. HOSONO, *Traveling waves for the Lotka-Volterra predator-prey system without diffusion of the predator*, Discrete Contin. Dyn. Syst. Ser. B, 20 (2015), pp. 161–171.

[39] S. R. DUNBAR, *Traveling waves in diffusive predator-prey equations: Periodic orbits and point-to-periodic heteroclinic orbits*, SIAM J. Appl. Math., 46 (1986), pp. 1057–1078.

[40] J. M. FRAILE AND J. C. SABINA, *General conditions for the existence of a critical point–periodic wave front connection for reaction-diffusion systems*, Nonlinear Anal., 13 (1989), pp. 767–786.

[41] Y. HUANG AND P. WENG, *Periodic traveling wave train and point-to-periodic traveling wave for a diffusive predator-prey system with Ivlev-type functional response*, J. Math. Anal. Appl., 417 (2014), pp. 376–393.

[42] A. GHAZARYAN AND B. SANDSTEDE, *Nonlinear convective instability of Turing-unstable fronts near onset: A case study*, SIAM J. Appl. Dyn. Syst., 6 (2007), pp. 319–347.

[43] M. BECK, A. GHAZARYAN, AND B. SANDSTEDE, *Nonlinear convective stability of travelling fronts near Turing and Hopf instabilities*, J. Differential Equations, 246 (2009), pp. 4371–4390.

[44] J. A. SHERRATT, *Invasive wave fronts and their oscillatory wakes are linked by a modulated travelling phase resetting wave*, Phys. D, 117 (1998), pp. 145–166.

[45] J. A. SHERRATT, M. J. SMITH, AND J. D. M. RADEMACHER, *Locating the transition from periodic oscillations to spatiotemporal chaos in the wake of invasion*, Proc. Natl. Acad. Sci. USA, 106 (2009), pp. 10890–10895.

[46] A. S. DAGBOVIE AND J. A. SHERRATT, *Absolute stability and dynamical stabilisation in predator-prey systems*, J. Math. Biol., 68 (2014), pp. 1403–1421.

[47] M. J. SMITH AND J. A. SHERRATT, *Propagating fronts in the complex Ginzburg-Landau equation generate fixed-width bands of plane waves*, Phys. Rev. E, 80 (2009), 046209.

[48] J. E. BROMMER, H. PIETIÄINEN, K. AHOLA, P. KARELL, T. KARSTINEN, AND H. KOLUNEN, *The return of the vole cycle in southern Finland refutes the generality of the loss of cycles through "climatic forcing,"* Glob. Change Biol., 16 (2010), pp. 577–586.

[49] R. A. IMS, J. A. HENDEN, AND S. T. KILLENGREEN, *Collapsing population cycles*, Trends Ecol. Evol., 23 (2008), pp. 79–86.

[50] M. L. ROSENZWEIG AND R. H. MACARTHUR, *Graphical representation and stability conditions of predator-prey interactions*, Am. Nat., 97 (1963), pp. 209–223.

[51] F. LUTSCHER, E. PACHEPSKY, AND M. A. LEWIS *The effect of dispersal patterns on stream populations*, SIAM J. Appl. Math., 65 (2005), pp. 1305–1327.

[52] J. MEDLOCK AND M. KOT, *Spreading disease: Integro-differential equations old and new*, Math. Biosci., 184 (2003), pp. 201–222.

[53] M. A. GILBERT, S. M. WHITE, J. M. BULLOCK, AND E. A. GAFFNEY, *Spreading speeds for stage structured plant populations in fragmented landscapes*, J. Theoret. Biol., 349 (2014), pp. 135–149.

[54] S. PETROVSKII, A. MOROZOV, AND L. BAI-LIAN, *On a possible origin of the Fat-tailed dispersal in population dynamics*, Ecol. Complex., 5 (2008), pp. 146–150.

[55] S. PETROVSKII AND A. MOROZOV, *Dispersal in a statistically structured population: Fat tails revisited*, Am. Nat., 173 (2009), pp. 278–289.

[56] M. KOT, M. A. LEWIS, AND P. VAN DEN DRIESSCHE, *Dispersal data and the spread of invading organisms*, Ecology, 77 (1996), pp. 2027–2042.

[57] J. SUGIE AND Y. SAITO, *Uniqueness of limit cycles in a Rosenzweig-MacArthur model with prey immigration*, SIAM J. Appl. Math., 72 (2012), pp. 299–316.

[58] R. WEINER, B. A. SCHMITT, AND H. PODHAISKY, *ROWMAP—a ROW-code with Krylov techniques for large stiff ODEs*, Appl. Numer. Math., 25 (1997), pp. 303–319.

[59] J. A. SHERRATT, *Oscillatory and chaotic wakes behind moving boundaries in reaction-diffusion systems*, Dyn. Stab. Systems, 11 (1996), pp. 303–325.

[60] S. V. PETROVSKII AND H. MALCHOW, *A minimal model of pattern formation in a prey-predator system*, Math. Comput. Modelling, 29 (1999), pp. 49–63.

[61] S. V. PETROVSKII AND H. MALCHOW, *Wave of chaos: New mechanism of pattern formation in spatio-temporal population dynamics*, Theor. Pop. Biol., 59 (2001), pp. 157–174.

[62] W. VAN SAARLOOS, *The complex Ginzburg-Landau equation for beginners*, in Spatio-temporal Patterns in Nonequilibrium Complex Systems, P. E. Cladis and P. Palffy-Muhoray, eds., Santa Fe Institute, Studies in the Sciences of Complexity, Proceedings 21, Addison-Wesley, Reading, MA, 1994, pp. 19–31.

[63] V. GARCÍA-MORALES AND K. KRISCHER, *The complex Ginzburg-Landau equation: An introduction*, Contemp. Phys., 53 (2012), pp. 79–95.

[64] Y. KURAMOTO, *Scaling behavior of turbulent oscillators with non-local interaction*, Progr. Theoret. Phys., 94 (1995), pp. 321–330.

[65] D. TANAKA AND Y. KURAMOTO, *Complex Ginzburg-Landau equation with nonlocal coupling*, Phys. Rev. E, 68 (2003), 026219.

[66] V. GARCÍA-MORALES, R. W. HÖLZEL, AND K. KRISCHER, *Coherent structures emerging from turbulence in the nonlocal complex Ginzburg-Landau equation*, Phys. Rev. E, 78 (2008), 026215.

[67] V. GARCÍA-MORALES AND K. KRISCHER, *Nonlocal complex Ginzburg-Landau equation for electrochemical systems*, Phys. Rev. Lett., 100 (2008), 054101.

[68] J. A. SHERRATT AND M. J. SMITH, *Periodic travelling waves in cyclic populations: Field studies and reaction-diffusion models*, J. R. Soc. Interface, 5 (2008), pp. 483–505.

[69] G.-B. ZHANG, W.-T. LI, AND Z.-C. WANG, *Spreading speeds and traveling waves for nonlocal dispersal equations with degenerate monostable nonlinearity*, J. Differential Equations, 252 (2012), pp. 5096–5124.

[70] F.-Y. YANG, W.-T. LI, AND Z.-C. WANG, *Traveling waves in a nonlocal dispersal SIR epidemic model*, Nonlinear Anal. Real-world Appl., 23 (2015), pp. 129–147.

[71] Y. A. KUZNETSOV, *Elements of Applied Bifurcation Theory*, Springer-Verlag, New York, 2004.

[72] J. A. SHERRATT, X. LAMBIN, AND T. N. SHERRATT, *The effects of the size and shape of landscape features on the formation of traveling waves in cyclic populations*, Am. Nat., 162 (2003), pp. 503–513.

[73] J. A. SHERRATT, *Numerical continuation methods for studying periodic travelling wave (wavetrain) solutions of partial differential equations*, Appl. Math. Comput., 218 (2012), pp. 4684–4694.

[74] J. D. M. RADEMACHER, B. SANDSTEDE, AND A. SCHEEL, *Computing absolute and essential spectra using continuation*, Phys. D, 229 (2007), pp. 166–183.

[75] J. A. SHERRATT, *Numerical continuation of boundaries in parameter space between stable and unstable periodic travelling wave (wavetrain) solutions of partial differential equations*, Adv. Comput. Math., 39 (2013), pp. 175–192.

[76] M. KOT, *Discrete-time travelling waves: ecological examples*, J. Math. Biol., 30 (1992), pp. 413–436.

[77] T. N. SHERRATT, X. LAMBIN, S. J. PETTY, J. L. MACKINNON, C. F. COLES, AND C. J. THOMAS, *Application of coupled oscillator models to understand extensive synchrony domains and travelling waves in populations of the field vole in Kielder forest, UK*, J. Appl. Ecol., 37 (2000), pp. 148–158.

[78] J. A. SHERRATT, *Periodic travelling waves in a family of deterministic cellular automata*, Phys. D, 95 (1996), pp. 319–335.

[79] P. W. BATES AND G. ZHAO, *Existence, uniqueness and stability of the stationary solution to a nonlocal evolution equation arising in population dispersal*, J. Math. Anal. Appl., 332 (2007), pp. 428–440.

[80] J. W. SUN, *Existence and uniqueness of positive solutions for a nonlocal dispersal population model*, Electron. J. Differential Equations, 2014.143 (2014), pp. 1–9.

[81] J. W. SUN, F. Y. YANG, AND W. T. LI, *A nonlocal dispersal equation arising from a selection-migration model in genetics*, J. Differential Equations, 257 (2014), pp. 1372–1402.